KLOE NOTE n^{o}205
September 2005

Measurement of the branching ratio of the $K^+ \to \mu^+\nu(\gamma)$ decay

E. De Lucia[a], **R. Versaci**[b]

[a]Laboratori Nazionali di Frascati dell'INFN
[b]Institut für Experimentelle Kernphysik, Universität Karlsruhe, Germany

Abstract

We present the measurement of the fully inclusive $K^+ \to \mu^+\nu(\gamma)$ absolute branching ratio. For this measurement about 175 pb^{-1} of total integrated luminosity of 2002 data have been used. Using a sample of $\sim 10^5$ $K^+ \to \mu^+\nu(\gamma)$ decays we have found $BR(K^+ \to \mu^+\nu(\gamma)) = 0.6366 \pm 0.0009_{\text{stat.}} \pm 0.0015_{\text{syst.}}$, corresponding to an overall fractional error of 0.27%. We obtain an estimate for the CKM mixing matrix element $|V_{us}| = 0.2223 \pm 0.0026$, using recent lattice results on the decay constants of pseudoscalar mesons.

1 Introduction

An inspection of The Particle Data Group Review of 2004 [1], clearly reveals that most branching ratios, BR, for the principal decay modes of the charged kaons were performed last in the early seventies. The most recent measurement of the $K \to \mu\nu$ branching ratio [2], based on 72,000 events, dates back to 1972 and relies on a sample of $\sim 10^5$ kaon decays. The authors of [2] quote an error of $\sim 0.7\%$, the statistical error due to the event count being 0.4%. This error is reduced in the PDG fit to 0.27% and the value changed by 0.3%. While the procedure is correct in principle, it can lead to incorrect results because of incorrect data included in the fit. This has been the case sometimes, leading among other things to the suggestion, also in [1], of a value for $|V_{us}|$ apparently inconsistent with unitarity of the CKM mixing matrix [3].

Another problem with measurements performed more than 30 years ago is due to the fact that the importance of radiative corrections was not fully appreciated. It is therefore impossible to understand what fraction of the radiative decay is included in the quoted result. Inclusion of all radiation is however necessary to compare to models or to extract fundamental parameters such as a coupling constant. With all the above in mind as well as recent developments in numerical or lattice QCD calculation, we have begun a program of new precise, fully inclusive, kaon branching ratios.

In the following we report the measurement of $K^+ \to \mu^+\nu(\gamma)$.

2 Analysis scheme

The procedure of this analysis can be summarized as follows:

1. Selection of a pure "K^+ beam" using the tag algorithm (see section 4).
2. Production of the momentum spectrum of the charged secondary in the kaon rest frame (see section 5).
3. Selection of the spectrum of the background events, which is made of $K_{\pi 2}$, $K_{\mu 3}$, K_{e3}, $K_{\pi 3}$ decays and its subtraction from the signal spectrum (see section 6).
4. Counting of the signal events, after the subtraction.
5. Normalization with respect to the number of tags (i.e. number of K^+). This provides a *first estimate* $BR_0 = N_{K^+ \to \mu^+\nu(\gamma)}/\ N_{TAG}$ which must be corrected for detection efficiency ϵ.
6. Evaluate, from data, the DC reconstruction efficiency of a signal event. The efficiency is corrected to take in account a small discrepancy between the true and the reconstructed MC efficiencies. (see section 7).

7. Correct the branching ratio for the tag bias $C_{\rm TB}$ (see section 8.1), the cosmic-ray veto $C_{\rm CRV}$ and the filfo filter $C_{\rm FF}$ (see section 9)

8. Evaluate the systematics of this measurement. (see section 9).

Following this scheme the branching ratio is given by:

$$BR\left(K^+ \to \mu^+\nu(\gamma)\right) = \frac{N_{K^+\to\mu^+\nu(\gamma)}}{N_{TAG}} \times \frac{1}{\epsilon\, C_{\rm CRV}\, C_{\rm FF}\, C_{\rm TB}} \tag{1}$$

where $N_{K^+\to\mu^+\nu(\gamma)}$ are the events selected as signal (hereafter signal count), N_{Tag} is the number of tagged events and ϵ is the acceptance. $C_{\rm CRV}$ and $C_{\rm FF}$ are the corrections for the effects due to the cosmic-ray veto and the filfo procedure, and $C_{\rm TB}$ accounts for the tag bias effect.

3 The data sample

The sample used for this analysis has been collected during 2002 data taking, processed and filtered with the KLOE standard reconstruction software and the event classification procedure. We split the data in two samples of about 60 pb^{-1} and 115 pb^{-1}; the former has been used for the measurement of the *first estimate*, the latter has been used to evaluate the efficiency and the background. A 1:1 Monte Carlo simulation has been produced and used. The whole simulation has been used for the tag bias evaluation.

4 Selection of the self-triggering tag events

The peculiarity of a ϕ-factory is that kaons are produced in pairs K^+K^- and K_LK_S. Therefore the detection of a K guarantees the presence of a $\bar{K}$ on the other side with known momentum and direction. This feature allows the measurement of absolute branching ratios. The decay products of the K^+K^- pair define two spatially well separated regions called in the following the tag and the signal hemispheres.
To measure absolute branching ratios we consider the subsample of events selected by the TAG algorithm (see section 4.1). Once the algorithm has found a $K^\mp$ tag decay, it can be used as reference normalization and the kaons in the other hemisphere can be considered as a pure $K^\pm$ beam. In the two-body decays the secondary tracks have a well defined momentum in the kaon rest frame and this allows a good particle identification. To minimize the impact of the trigger efficiency on the signal side, we look for a tag decay which also provided by itself the EMC trigger of the event.
Even if the analyzed events already belong to the charged kaons stream, it is necessary to reprocess them for the following reasons: to tighten the requirements on the tag decay, cleaning the data sample, and to select a specific charge for the self-triggering tags (see section 4.2).

In the following we use a coordinate system with the z-axis defined as the bisectrix of the beams, the y-axis vertical and the x-axis toward the center of the collider rings.

4.1 The TAG algorithm

The TAG algorithm tries to identify the two-body decays $K \to \mu\nu$ or $K \to \pi\pi^0$, which are about 85% of charged kaon decays. It requires two tracks connected to the same vertex. As first a track (kaon candidate) with the point of closest approach to the IP smaller than $d_0 = 10$ cm ($z_0 = 20$ cm) along the radial (longitudinal) axis is required. The radial distance between the kaon candidate decay vertex and the beam axis, R_V, has to fulfill $40 < R_V < 150$ cm. The kaon candidate must also have $70 < |\overrightarrow{p}| < 130$ MeV/c. Once the kaon candidate has been identified:

- the candidate secondary track must have the same charge of the kaon;
- the momentum difference between the kaon and the secondary must fulfill $-320 < \Delta p = |\overrightarrow{p}_K| - |\overrightarrow{p}_{sec}| < -120$ MeV/c;
- the secondary momentum in the kaon rest frame, p^*, using the $\pi^\pm$ mass hypothesis, must be in the range $180 < p^* < 270$ MeV/c.

After the preliminary kaon decay vertex selection a tighter cut on the secondary track momentum in kaon rest frame is applied to distinguish between K_μ and $K_{\pi\pi^0}$ decays:

$$225 < p^* < 245 \text{ MeV/c} \quad \Rightarrow \quad K_\mu\text{-tag} \tag{2}$$

$$195.5 < p^* < 213.5 \text{ MeV/c} \quad \Rightarrow \quad K_{\pi\pi^0}\text{-tag.} \tag{3}$$

4.2 Self-triggering conditions

Given the two-body decay selected by the tag algorithm, we require that the clusters associated with the tag provide an EMC trigger (self-triggering tag). The EMC trigger is given by two energy deposits in two trigger sectors which overcome the LET threshold [4], whose value corresponds to an average value approximately equal to 50 MeV in the barrel and 150 MeV in the endcaps.
The possibility for a K_μ decay to self-trigger the event is due to the cluster associated to the secondary $\mu^\pm$ track. The trajectory of the $\mu^\pm$ in the EMC can cross two adjacent trigger sectors. If the two energy deposits are over threshold we have a self-triggering K_μ decay event. The self-triggering request reduces the analysis sample. The yield has been evaluated on a 4.85 pb^{-1} data sample. The results are reported in table 1. The amount of self-triggering K_μ tag decays is about 35%.
In the case of $K_{\pi\pi^0}$ tag decay the amount of self-triggering event is about 75%; this

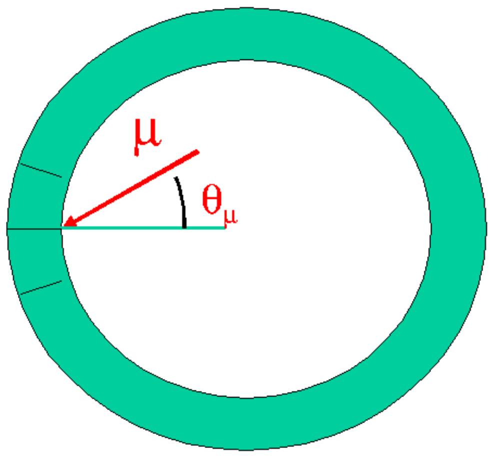

Figure 1: Schematic geometrical overview of a K_μ self-triggering event. Depending on the incidence angle θ_μ, the muon can cross two trigger sectors and then self-trigger the event.

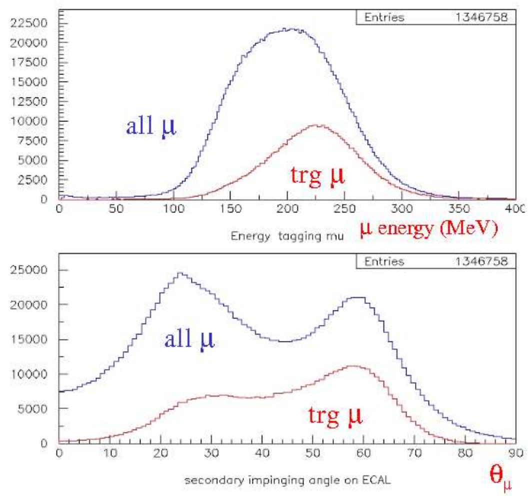

Figure 2: Above: distribution of self-triggering muon as function of the energy released by the muon in the calorimeter. Below: distribution of self-triggering muon as function of its impinging angle on the EMC.

Kind of tag	Number of tags pb^{-1}	Number of self-trigger pb^{-1}
$K^- \rightarrow \mu^- \bar{\nu}$	279×10^3	95×10^3
$K^- \rightarrow \pi^- \pi^0$	95×10^3	73×10^3

Table 1: Number of self-triggering tag events per pb^{-1}, evaluated using a data sample of about 4.85 pb^{-1}

is due to the fact that either the charged pion or the photons from the π^0 decay can overcome the calorimeter energy threshold.

We require self-triggering tags for every sample used in this analysis. It must be stressed that after the self-triggering tag request, we end up on the opposite hemisphere with a pure $K^\pm$ beam.

5 Selection of the events

Since the nuclear cross-section of a positive kaons is reduced by a factor of about 10^2 with respect to that of a negative kaon, only events with K^- tag and with K^+ on the signal hemisphere have been used. This is done in order to avoid distortion of the branching ratio due to nuclear interactions of the kaons.
A signal K^+ event is defined by the following requests:

- a negative kaon giving the self-triggering tag;
- a positive kaon defined as that one of the kaon tag:

$$R_{PCA} < 10 \text{ cm} \qquad \text{where} \qquad R_{PCA} = \sqrt{x_{PCA}^2 + y_{PCA}^2}, \tag{4}$$

$$|Z_{PCA}| < 20 \text{ cm}, \tag{5}$$

$$70 < P_K < 130 \text{ MeV/c}; \tag{6}$$

- a decay vertex defined as that one of the kaon tag:

$$40 < R_V < 150 \text{ cm}; \tag{7}$$

- events with backward reconstructed kaon are rejected;
- the kaon on the signal hemisphere is extrapolated backward up to the IP taking into account the energy loss. The aim of the extrapolation is to clean the sample and to allow the reconstruction of the timing of the event, which is necessary for the background selection.

In figure 3 is shown the resulting spectrum of the momenta of the charged secondary in the kaon rest frame, for the entire Monte Carlo sample. This spectrum has two peaks, the first at about 236 MeV/c, due to the two body decay $K^+ \rightarrow \mu^+\nu$

and the second peak at about 205 MeV/c due to the $K^+ \rightarrow \pi^+\pi^0$ decay; lower momenta are due to three body decays.
All the momenta of the charged secondaries produced in the kaon decay are evaluated hereafter in the kaon rest frame and in the hypothesis of pion mass. Since in the case of the peak at 205 MeV we are using the correct value for the mass, we obtain a symmetric peak. The peak at 236 MeV instead is not symmetric because it has been reconstructed in the wrong mass hypothesis (pion instead of muon).
Since we are interested in $K^+ \rightarrow \mu^+\nu(\gamma)$ only, the remaining decays are the background and a method to subtract it must be implemented.

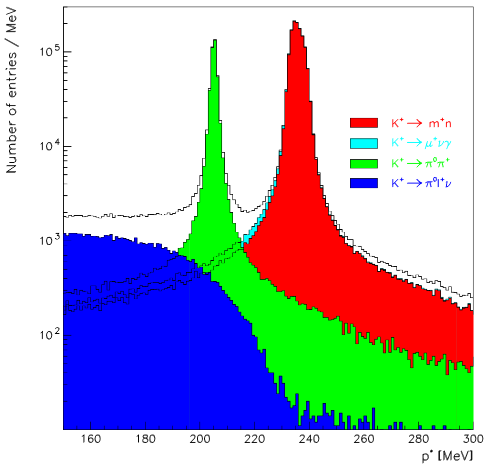

Figure 3: Monte Carlo spectra of the charged decay particle momentum transformed to the kaon rest frame, assuming the pion mass. The two peaks corresponds to pions from $K^+ \rightarrow \pi^+\pi^0$, at 205 MeV/c and $K^+ \rightarrow \mu^+\nu$ at 236 MeV. Contributions from $K^+ \rightarrow \mu^+\nu\gamma$ are also shown.

6 Background evaluation

The $K^+ \rightarrow \pi^+\pi^+\pi^-$ and $K^+ \rightarrow \pi^+\pi^0\pi^0$ decays do not contribute to the background because the maximum momentum of a pion produced in these decays is 125 MeV, therefore the contribution to the spectrum above 200 MeV is negligible. In all the remaining non-$K^\pm \rightarrow \mu^\pm\nu$ kaon decays ($K^+ \rightarrow \pi^+\pi^0$, $K^+ \rightarrow \pi^0\mu^+\nu$, $K^+ \rightarrow \pi^0 e^+\nu$, $K^+ \rightarrow \pi^+\pi^0\pi^0$), a neutral pion is always produced. This allows us to define as background all the events which have a π^0 among the decay products.
The Monte Carlo momentum spectrum of the charged secondary for this kind of decay is shown in figure 4 left.

6.1 The π^0 definition

The preliminary requirement to find an event with a π^0 ($X\pi^0$-event) is the presence of at least two not associated clusters (if there are more than two clusters we consider the most energetic) with:

- $24° < \alpha_{cl} < 156°$;
- $\tau_\phi < t_{cl} < \tau_\phi + 55$ ns ;

where α_{cl} is the angle between the direction of the cluster and the z axis, and t_{cl} is the time of the cluster.

Then at least a pair of these clusters must fulfill two requirements on the timing and on the π^0 candidate invariant mass.
The invariant mass is defined as:

$$M_{\pi^0} \ = \ \sqrt{2 \cdot E_{cl_1} \cdot E_{cl_2} \cdot (1 - \cos\theta)} \tag{8}$$

where θ is the angle between the directions of the two photons produced in the π^0 decay, and E_{cl_1} E_{cl_2} are the energies of the neutral clusters fired by the photons. The direction of the photon is defined as the vector from the kaon decay vertex to the neutral cluster in EMC.
M_{π^0} must be in the range: $80 < M_{\pi^0} < 200$ MeV.
For the timing we have to define first the difference

$$\Delta t = \left(t_{cl_1} - \frac{\Delta x_1}{c}\right) - \left(t_{cl_2} - \frac{\Delta x_2}{c}\right) \tag{9}$$

where t_{cl_i} is the time of the neutral cluster and Δx_i is the distance between the neutral cluster and the kaon vertex.
The requirement for the timing is $(|\Delta t|/\sigma_t) < 5$, where the global time resolution $\sigma_t = \sqrt{\sigma_{t_1}^2 + \sigma_{t_2}^2}$ is defined as

$$\sigma_{t_i} = C_1 + \frac{C_2}{\sqrt{E_{cl_i}(GeV)}} \tag{10}$$

with $C_1 = 140$ ps is a constant term connected to the bunch length and to the electronic, and $C_2 = 57$ ps is a stochastic term due to calorimeter resolution.

If both requirements described above are satisfied, a π^0 has been detected, and a χ^2 is evalated for systematics purposes.
The χ^2 is defined as:

$$\chi^2 = \left(\frac{M_{\pi^0} - M_{\pi^0}^{PDG}}{\sigma_{mass}}\right)^2 + \left(\frac{\Delta t}{\sigma_t}\right)^2 \tag{11}$$

where $M_{\pi^0}^{PDG} = 134.9766$ [1] and $\sigma_{mass} = 17$ MeV.
The χ^2 distribution is shown in figure 4 right.

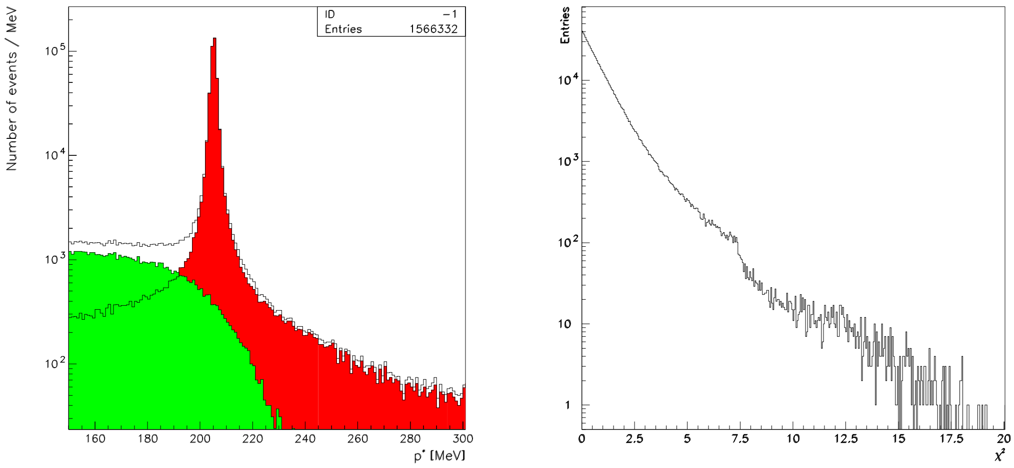

Figure 4: Left: Monte Carlo spectra of the charged decay particle momentum transformed to the kaon rest frame, assuming the pion mass, for background events. Right: χ^2 distribution for the reconstructed $X\pi^0$ events.

6.2 Background subtraction

The background spectrum and the spectrum of the $K^+ \to \mu^+\nu$, obtained from the efficiency sample (see section 7), are used together to fit the distribution of the momentum of the charged secondary (see figure 5 left).
The aim of the fit is to obtain a scale factor for the background spectrum, in order to subtract it from the signal.
Monte Carlo studies have shown a small discrepancy between the tails of the true ($X\pi^0$-events selected by kine, MC_{true}) background spectrum and of the spectrum of $X\pi^0$-events selected with the same procedure used on data ($MC_{reconstructed}$) has been seen. In order to take care of this small discrepancy we apply a correction consisting of a bin by bin ratio of the two Monte Carlo spectra, true over reconstucted:

$$DATA_{corrected} = DATA_{uncorrected} \cdot \frac{MC_{true}}{MC_{reconstructed}} \tag{12}$$

Then we can obtain $N_{K^+\to\mu^+\nu(\gamma)}$ performing the sum of the events included in the range $[p^*_{min}, p^*_{Max}]$ (see figure 5 right). We chose $p^*_{min} = 225$ MeV in order to keep as much events as possible without getting close the pion peak and being sensitive to the resolution effect. For the higher extreme of the sum we choise $p^*_{Max} = 400$ MeV.

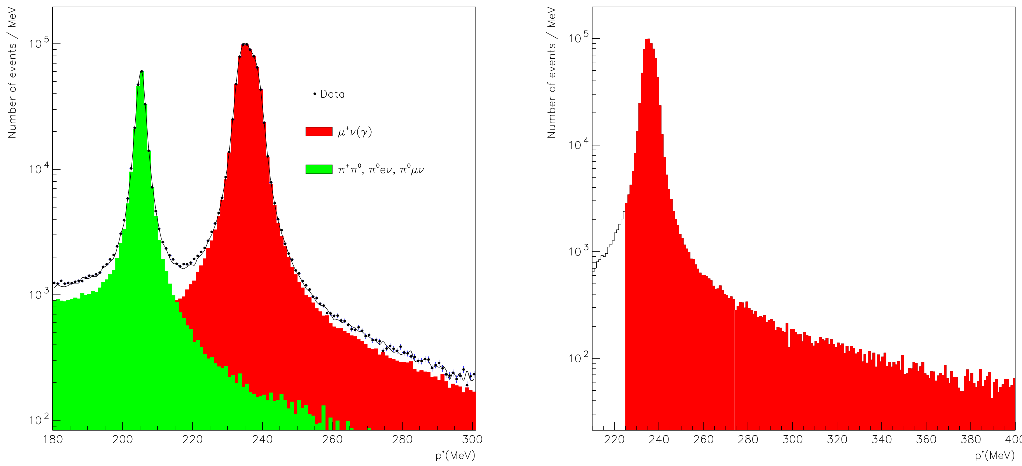

Figure 5: Left: Spectra of the charged-secondary momentum in the kaon rest frame for data. The solid line indicates the fit done with a linear combination of signal and background distributions obtained from data. Right: The same spectra after background subtraction. The range used for counting $K^+ \to \mu^+\nu(\gamma)$ events is indicated.

7 Efficiency evaluation

The reconstruction efficiency of a $K^+ \to \mu^+\nu(\gamma)$ event in the drift chamber with $p^*_{min} < p^* < p^*_{Max}$ is the convolution of the DC tracking efficiency for the kaon and the secondary track, times the vertex efficiency. To avoid correlation with the DC driven sample selection, we evaluate the global efficiency ϵ using mainly EMC information.

7.1 Preselection of the efficiency sample

$K^+ \to \mu^+\nu(\gamma)$, $K^- \to \mu^-\overline{\nu}(\gamma)$ events (hereafter $K_{\mu\mu}$ events) have a typical signature in EMC. They fire only two clusters with energy higher than $\sim$ 80 MeV. This provides the opportunity to evaluate the reconstruction efficiency of $K^\pm \to \mu^\pm\nu(\gamma)$ using only EMC information to select the control sample.
The first requirement is the presence of a self-triggering negative K_μ-tag in order to have homogeneous signal and efficiency samples.
Then we consider events with only one cluster fired excluding the cluster responsible for the trigger and excluding clusters having energy below 20 MeV (hereafter Low Energy Cut). We stress that we don't require the association between this cluster and any track. The LEC accounts for low energy clusters (few tens of MeV), due to machine background or cluster splitting and for photons from $K^\pm \to \mu^\pm\nu\gamma$ which

can be present.
After these cuts we obtain the cluster energy distribution reported in figure 6.

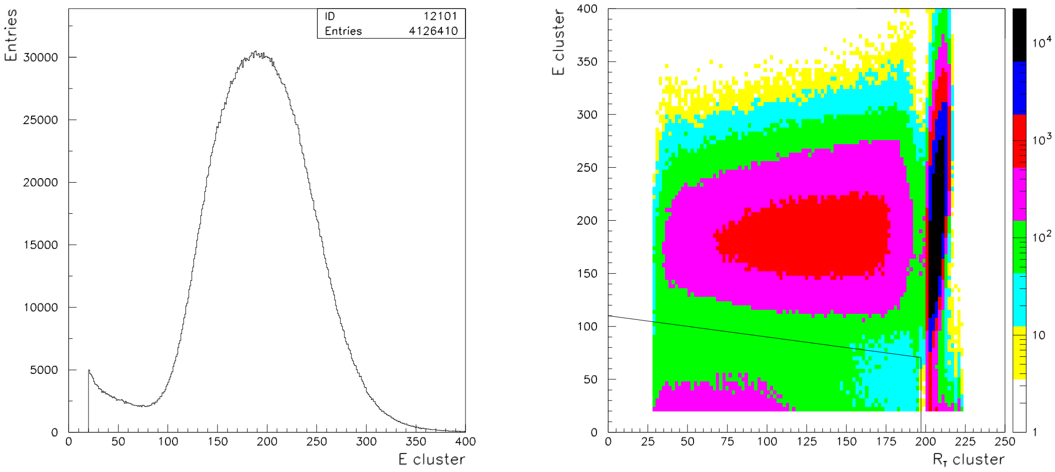

Figure 6: On the left is shown the energy spectrum of the second cluster after first step of the calorimeter preselection. On the right is shown the distribution of the second cluster as function of the energy and the radius of the cluster. The black line represent the cut applied in order to get rid of accidental clusters. Clusters below the line are rejected.

To get rid of high energy machine background and cluster splitting another cut has been applied. The cluster has to be in the barrel $R_{\rm xy} > 197$ cm or to satisfy the requirement on the cluster energy $E_{\rm cl}$, and on the transverse radius of the cluster $R_{\rm xy}$ $(E_{\rm cl}/(GeV) + R_{\rm xy}/5(cm) \geq 110)$. Moreover as final cut for the efficiency evaluation we require $E_{cl} \geq 80$ MeV (hereafter High Energy Cut).
The events fulfilling this calorimetric preselection constitute the efficiency sample: $N^{\mu\mu}_{TAG}$. Then we apply the signal selection, described in section 5, to this data sample.
The efficiency is defined as the ratio of $N_{K^+\to\mu^+\nu(\gamma)}$, number of signal events in the efficiency sample in the range $[p^*_{min}, p^*_{Max}]$ MeV/c, over $N^{\mu\mu}_{TAG}$:

$$\epsilon = \frac{N_{K^+\to\mu^+\nu(\gamma)}}{N^{\mu\mu}_{TAG}} \tag{13}$$

The composition of the denominator has been studied on Monte Carlo simulation. These studies have shown the simultaneous presence of a pollution of about 1.2% and of a depauperation of the $K^+ \to \mu^+\nu$ signal sample. The pollution is mainly due to $K^+ \to \pi^+\pi^+\pi^-$ and to misreconstructed $K^+ \to \pi^+\pi^0$. These two components cancel out at the level of $\mathcal{O}(10^{-4})$.

The procedure to measure the efficiency relies on the assumption that the DC efficiency to reconstruct a $K \to \mu\nu(\gamma)$ event on all the data set is well reproduced by the DC reconstruction efficiency from the $K_{\mu\mu}$ sample. The spectrum of the $K \to \mu\nu(\gamma)$ events selected by the EMC must be substantially equal to the spectrum of the signal. This item has been studied on the Monte Carlo simulation and in figure 7 are shown the comparisons between the two normalized spectra.

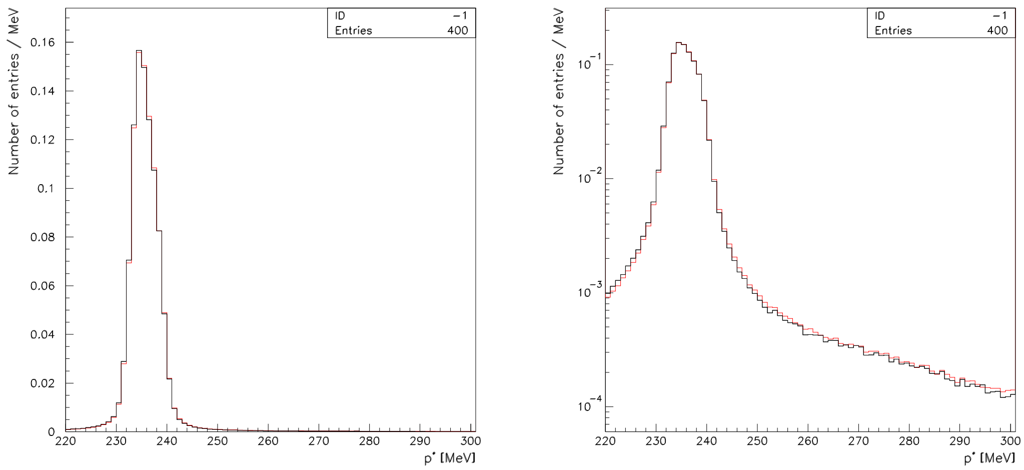

Figure 7: In figure are shown the spectra of muons selected by Monte Carlo true (black) and using calorimeter requirements (red).

7.2 Comparison with Monte Carlo simulation

To take care of second order correction to the efficiency, we have compared the efficiency measured on the Monte Carlo sample, treated like data i.e. using the calorimeter selection, with the efficiency measured on the "true" $K_{\mu\mu}$ Monte Carlo sample, selected looking at the Monte Carlo truth. A small discrepancy (of the order of 0.1%) has been observed. This is due to an excess of accidental clusters in the Monte Carlo simulation with respect to data, as can be seen in the left side of figure 8.

In order to get rid of this discrepancy we applied to the Monte Carlo events a smearing and a shift of the energy of the cluster. After the event has fulfilled the first requirement on two cluster fired, the energy of the second cluster (not the triggering) is changed according to the law:

$$E_{corrected} = E_{cl} + E_{shift} + A \cdot \sigma_{smear}$$

where E_{cl} is the energy of the cluster, $E_{shift} = -1.8\ MeV$ is the energy shift of the central values of the two distribution, A is a random parameter extracted according

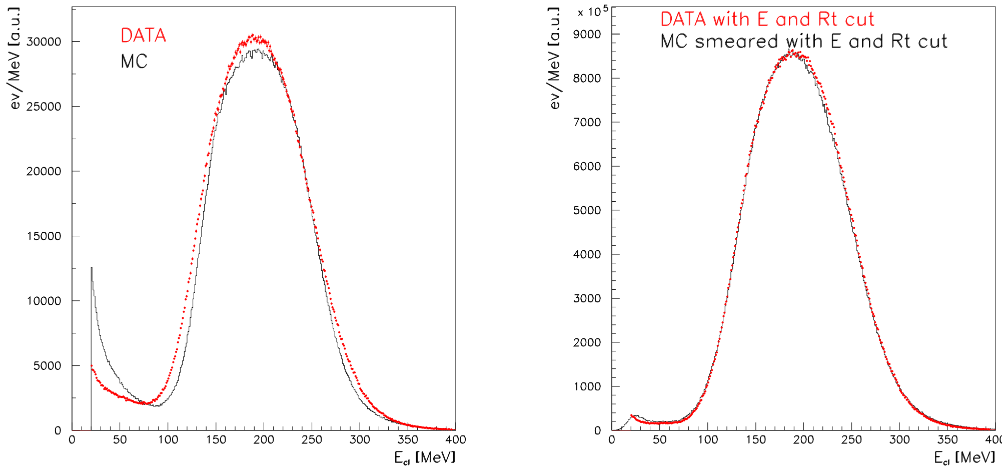

Figure 8: In figure are shown the spectra of muons selected by Monte Carlo true (black) and using calorimeter requirements (red).

to a gaussian distribution with $r.m.s. = 1$ and $\sigma_{smear} = 18 \cdot \sqrt{E_{cl}/195}$ MeV is the sigma of the cluster energy distribution which is centered at about 195 MeV. After this procedure the agreement between the Monte Carlo and the data distribution is greatly improved (see the right side of figure 8), and the previous discrepancy between the evaluated and the true efficiency is negligible. Nonetheless we apply the following correction to the evaluated efficiency: $\epsilon_{corr} = \epsilon_{true}/\epsilon$, where ϵ_{true} is the true MC efficiency and $\epsilon_{corr} \simeq 0.9988$.

Moreover this correction takes care also of the effect of the pollution and the depauperation of the efficiency sample previously discussed. We have studied the stability of this cancellation among systematic effects for the efficiency. The correction is highly sensitive to the LEC choosen. The pollution goes from a value of about 0.7% (LEC=10 MeV) up to about 3% (LEC=40 MeV). The correction spans in the same range and the corrected efficiency changes of about 5×10^{-4}.

Lately a study of the sensitivity of the measurement to the kaon lifetime used in the Monte Carlo simulation has been performed. We selected two subsamples of Monte Carlo events with lifetime changed of $\pm 10\%$. For both subsamples the value of the correction has changed of less than 10^{-4}, corresponding to a change on the branching ratio of $< 10^{-6}$.

8 Branching ratio calculation

8.1 Tag bias

There is a further correction needed to estimate the $K^+ \to \mu^+\nu(\gamma)$ branching ratio: this correction is due to the bias on the signal sample induced by the tag selection, and is called tag bias.
To evaluate the tag bias we used the Monte Carlo. We selected events tagged by a negative self-triggering $K^- \to \mu^-\overline{\nu}$ tag as in the analysis, then we looked at the K^+ branching ratios distribution obtained from the Monte Carlo. It has been shown that, with respect to the generated ones, the branching ratios of $K^+ \to \mu^+\nu$ and $K^+ \to \pi^+\pi^0$ decays increase, while the branching ratios of the other decays decrease (see fig. 9).
This behaviour can be explained as follows: the low momentum tracks from three body decays on the signal side bend more in the magnetic field and overlap on the tag hemisphere tracks, with corresponding worsening of the reconstruction efficiency. Then we have less tag in case of three bodies decays on the signal hemisphere with respect to the two body decays case.
The so far evaluated branching ratio $\widetilde{BR}$ must be corrected for the tag bias effect. The correction is the ratio between the generated branching ratio and the one measured after the tag requirement, C_{TB}. Then the final branching ratio is given by:

$$BR = \widetilde{BR} \cdot \frac{1}{C_{TB}} = \widetilde{BR} \cdot \frac{1}{\frac{BR_{MC\ after\ tag}}{BR_{MC\ generated}}} \tag{14}$$

We have evaluated the tag bias using the whole Monte Carlo production (kpm04 1:1 MC production).
For the $K^+ \to \mu^+\nu(\gamma)$ decay the tag bias correction values: $C_{TB} = 1.0164 \pm 0.0002$ (only statistic).

8.2 Uncertainty on the branching ratio

The statistical uncertainty on the branching ratio has been calculated using the formula:

$$\left(\frac{\Delta BR}{BR}\right)^2 = \left(\frac{\Delta BR_0}{BR_0}\right)^2 + \left(\frac{\Delta\epsilon}{\epsilon}\right)^2 + \left(\frac{\Delta\epsilon_{corr}}{\epsilon_{corr}}\right)^2 + \left(\frac{\Delta TB}{TB}\right)^2 \tag{15}$$

where each term is calculated using binomial statistics:

$$\frac{\Delta x}{x} = \left(\frac{n}{T}\right)^{-1} \cdot \sqrt{\frac{n}{T} \cdot \left(1 - \frac{n}{T}\right) \cdot \frac{1}{T}} \tag{16}$$

where $x = n/T$, n is the number of good events and T is the number of total events. Using the quoted sample of Monte Carlo and data we have:

- the fractional uncertainty on the *fist estimate*: $\frac{\Delta BR_0}{BR_0} \simeq 9 \cdot 10^{-4}$; n is the number of selected $K^+ \rightarrow \mu^+\nu(\gamma)$ events, T is the number of negative self-triggering tag;

- the fractional uncertainty on the efficiency ϵ: $\frac{\Delta\epsilon}{\epsilon} \simeq 7 \cdot 10^{-4}$; n is the number of selected $K^+ \rightarrow \mu^+\nu(\gamma)$ events, T is the number of negative self-triggering tag, both evaluated on the efficiency sample;

- the fractional uncertainty on the correction to the efficiency is the sum of two terms: the fractional uncertainty on the efficiency evaluated on the Monte Carlo simulation and the fractional uncertainty evaluated using the Monte Carlo truth:
$$\left(\frac{\Delta\epsilon_{corr}}{\epsilon_{corr}}\right)^2 = \left(\frac{\Delta\epsilon_{MC}}{\epsilon_{MC}}\right)^2 + \left(\frac{\Delta\epsilon_{MC\ true}}{\epsilon_{MC\ true}}\right)^2 \tag{17}$$
which are respectively: $\frac{\Delta\epsilon_{MC}}{\epsilon_{MC}} \simeq 7 \cdot 10^{-4}$ and $\frac{\Delta\epsilon_{true}}{\epsilon_{true}} \simeq 5 \cdot 10^{-4}$;

- the fractional uncertainty on the tag bias: $\frac{\Delta TB}{TB} \simeq 2 \cdot 10^{-4}$; n is the number of $K^+ \rightarrow \mu^+\nu(\gamma)$ events with a self-triggering negative K_μ-tag, T is the total number of self-triggering negative K_μ-tag.

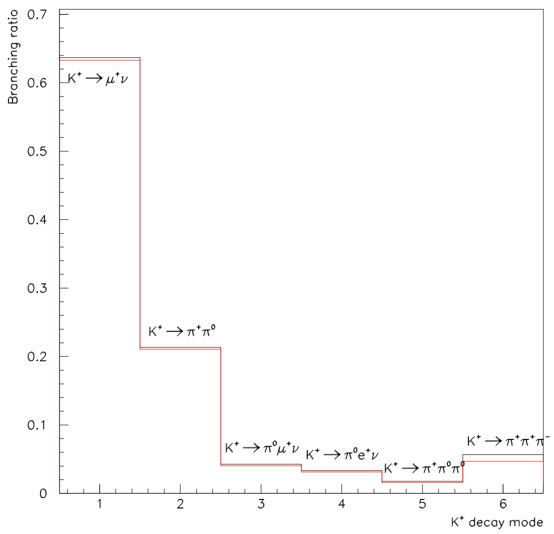

Figure 9: Comparison between the Monte Carlo generation branching ratios (black) and the branching ratio after the tag requirement (red), obtained using Monte Carlo truth. The effect of the "tag bias" is visible.

9 Study of the systematics

As consistency check, we have considered the difference between the branching ratio evaluated treating the Monte Carlo simulation like data, and the branching ratio inserted in the simulation at the generation level: $|BR_{MC\ recon.} - BR_{MC\ gen.}| = 10^{-4}$. Since it is well inside the statistical uncertainty we didn't taken into account this discrepancy as a systematic uncertainty.
We have studied the following sources of systematic uncertainties on the measured branching ratio:

1. low energy cut in efficiency evaluation;
2. high energy tail of radiative photons;
3. high energy cut in efficiency evaluation;
4. the fiducial volume for the vertex on the signal hemisphere;
5. the range of the fit of the background;
6. the cuts used to find the π^0 of the background spectrum;
7. the range of the signal region;
8. the requirements on the tag hemisphere;
9. the software veto FILFO [5], applied to filter out machine background and based on the topology and multiplicity of calorimeter clusters and drift chamber hits;
10. the cosmic-ray veto and T3 filter. Most of the Φ events rejected by the cosmic-ray veto are recovered by the third level trigger (called T3 filter) [5];
11. overlap of trigger sectors.

The associated systematic errors are listed in table 2.
We have also studied the branching ratio as a function of the time.

Efficiency low energy cut

This cut is strictly connected with the acceptance for an eventual γ from $K \to \mu\nu(\gamma)$. Increasing the low energy cut we could select events for the efficiency evaluation with more noise (i.e. machine background events). On the other hand also more $K^+ \to \mu^+\nu\gamma$ events are taken into account. We moved the cut from 10 to 40 MeV to check the stability of our result with respect to this cut. We quote as systematic uncertainty the difference between the highest and the lowest central value of the branching ratio we measured: $\delta_{LEC} = 5 \times 10^{-4}$.

High energy tail of radiative photons

The method used to count the $K \rightarrow \mu\nu(\gamma)$ signal events relies only on the DC identification of the kaon and muon tracks, so it is an inclusive measurement. Indeed the EMC selection of the sample used to measure the efficiency retains only those $K \rightarrow \mu\nu(\gamma)$ events whose reconstructed photon energy is smaller than E_{low}.
The high energy part of the spectrum of the radiative photon (see figure 10) is taken into account correcting the measured efficiency for MC.
A possible source of systematic uncertainty can be due to the Monte Carlo simulation of the high energy tail of $K^+ \rightarrow \mu^+\nu(\gamma)$ with $E_\gamma > E_{low}$.
The $K \rightarrow \mu\nu(\gamma)$ decay with $E_\gamma > 20\ MeV$ account for $(3.5 \pm\ 0.8) \times 10^{-3}$ [6] and if we assume a very conservative systematic uncertainty of the Monte Carlo simulation on this sample of events, $\simeq\ 20\%$, we end up with a systematic uncertainty due to the high energy radiative decay $\delta_{rad.}\ <\ 7 \times 10^{-4}$.
This value is in agreement with the one obtained using our Monte Carlo simulation for the radiative decay.

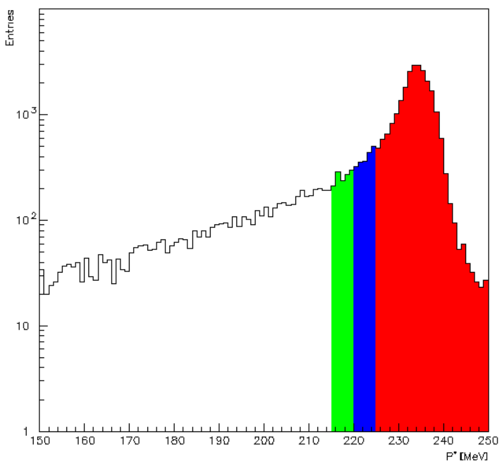

Figure 10: Spectrum of the muon from radiative $K^+ \rightarrow \mu^+\nu\gamma$ from reconstructed Monte Carlo. The red zone corresponds to the part of the spectrum of the $K^+ \rightarrow \mu^+\nu\gamma$ we take into account for the branching ratio measurement if $E_{low} = 10$ MeV. The zones in blue and green are added to the spectrum if we move E_{low} to 15 MeV and 20 MeV respectively.

Efficiency high energy cut

We evaluated this systematic uncertainty moving the High Energy Cut from 70 to 90 MeV, with a 5 MeV step. Defining the systematic uncertainty as done above, we quote: $\delta_{HEC}\ =\ 2 \times 10^{-4}$.

Fiducial volume

We changed the requirement on the minimum transverse radius of the kaon decay vertex on the signal side. The standard one is $40 < R_V < 150$ cm, we increased R_V up to 45 cm with a 1 cm step. Using our standard definition of systematic uncertainty we quote $\delta_{FV} = 5 \times 10^{-4}$.

Background fit range

We have performed the measurement of the branching ratio using different ranges for the fit of the signal spectrum (See section 6.2). The standard range is $[180, 300]$ MeV and we moved it with a 10 MeV step for both the high and the low extreme separately. Using our standard definition of systematic uncertainty we quote $\delta_{Fit} < 1 \times 10^{-4}$.

Background spectrum definition

We evaluated the systematic uncertainty on the measured branching ratio using as background shape the one obtained applying different cuts on the χ^2 defining the π^0. The background shapes have been obtained cutting 5%, 10%, 15%, 20% of the events with worst χ^2. The systematic uncertainty is $\delta_{\pi^0} = 3 \times 10^{-4}$.

Range of the signal region

We evaluated the systematic uncertainty on the branching ratio induced by different p^*_{min} and p^*_{Max} values. We moved p^*_{min} from 220 to 230 MeV/c increasing it with respect to the standard p^*_{min} value of 225 MeV/c. Actually it makes no sense lowering p^*_{min} due to the eventual uncertainties of the background subtraction around the $\pi\pi^0$ peak. We quote as systematic uncertainty $\delta_{p^*_{min}} = 3 \times 10^{-4}$.
p^*_{Max} has been moved from 300 to 400 MeV/c with a 20 MeV/c step, the systematic uncertaintiy is $\delta_{p^*_{Max}} < 1 \times 10^{-4}$.

Tag hemisphere

We have studied the variation of the branching ratio changing the cuts defining the tag. We moved separately the following cuts, previously enlarged with respect to the standard ones:

$$60 < P_K < 140\text{MeV/c}; \tag{18}$$
$$30 < R_V < 160 \text{ cm}; \tag{19}$$
$$150 < |p^*| < 300 \text{ MeV}; \tag{20}$$
$$-340 < \Delta p < -100 \text{ MeV}. \tag{21}$$

Therefore the systematic uncertainty coming from the tag definition is $\delta_{Tag} = 1 \times 10^{-4}$.

Nuclear interactions

The fraction of K^+ undergoing nuclear interaction has been evaluated using Monte Carlo. We assumed this value as upper bound for the systematic uncertainty on the measured branching ratio: $\delta_{NI} \; = \; 4 \times 10^{-4}$.

FILFO

The correction due to FILFO has been evaluted according to the formula:

$$C_{FILFO} = \alpha^{-1}_{FILFO} \tag{22}$$

where

$$\alpha_{FILFO} = \frac{1-\rho_{TAG}}{1-\rho^{SIG}_{TAG}} \qquad \text{and} \qquad \rho^i = \frac{N^i_{AFILFO}}{N^i_{FILFO} + N^i_{AFILFO}} \tag{23}$$

where N_{FILFO} and N_{AFILFO} are the events which satisfy and do not satisfy the FILFO requirements respectively; ρ is the FILFO inefficiency and it has been evaluated on two different samples, the first with the requirement of the tag only, the second requiring both the tag and the signal detection.
The FILFO correction has been evaluated both on data and Monte Carlo (in agreement within the error):

$$\alpha^{Data}_{FILFO} = 1.00006 \pm 0.00032 \tag{24}$$
$$\alpha^{MC}_{FILFO} = 0.99967 \pm 0.00015 \tag{25}$$

This leads to a negligible correction to the value of the branching ratio and contributes with an uncertainty of 3×10^{-4} to the total one.
The effect of FILFO on the BR measurement has been studied on control samples which do not undergo the FILFO filter. The same procedure has been applied to the cosmic-ray veto and T3 filter.

Cosmic-ray veto and T3 filter

The evaluation of the comsic-ray veto and T3 filter correction has been obtained directly from data using the ratio:

$$C_{CRV} = \frac{BR^{RAW}}{BR^{RAW}_{T3}} \tag{26}$$

where:

$$BR^{RAW} = \frac{N_{SIG}}{N_{TAG}} \qquad \text{and} \qquad BR^{RAW}_{T3} = \frac{N_{SIG} + 64 \times N^{T3flag=1}_{SIG}}{N_{TAG} + 64 \times N^{T3flag=1}_{TAG}} \tag{27}$$

The correction is $C_{CRV} \; = \; 1.0005 \pm 0.0003$ and introduces an uncertainty on the branching ratio of $\mathcal{O}(10^{-6})$.

Overlap of trigger sectors

The branching ratio has been measured both with and without the request of overlapping trigger sectors, using independent data samples. The difference among these two values is 0.0009, that is one standard deviation, and has been add to the list of systematic uncertainties.

Time stability

Finally we studied also the time stability of the branching ratio. We split the 2002 data sample in 11 subsamples of almost equal integrated luminosity and we measured the branching ratio for each of these. The time dependency is compatible with a constant function with $BR = 0.6366 \pm 0.0013$ value and $\chi^2/d.o.f. = 15.59/10$.

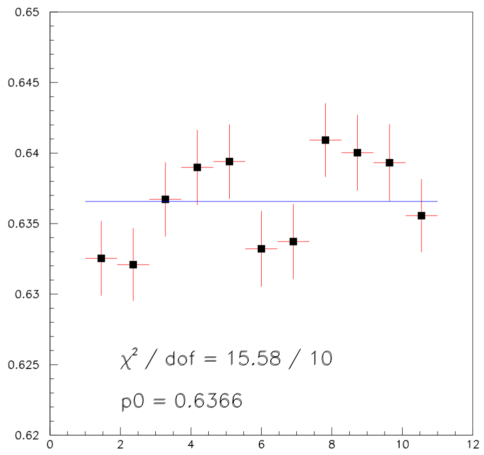

Figure 11: Behavior of the branching ratio as function of the time. The data sample has been split in subsamples having the same integrated luminosity. The result of a fit with a constant function is reported in figure.

10 Conclusions

On a sample of tagged events $N_{Tags} = 4,237,329$, we found a the number of signal events, with $225 \leq p^* \leq 400$ MeV/c, of $N_{K^+ \to \mu^+ \nu(\gamma)} = 865,283$. The efficiency measured directly on data is $\epsilon = 0.3153 \pm 0.0002$.
Using eq. 1, the absolute branching ratio is:

$$BR(K^+ \to \mu^+ \nu_\mu(\gamma)) = 0.6366 \pm 0.0009_{stat.} \pm 0.0015_{syst.} \tag{28}$$

Summary table of systematic uncertainties	
Source of systematic uncertainty	Value
$\delta_{Low\ Energy\ Cut}$	5×10^{-4}
$\delta_{High\ Energy\ Tail\ of\ radiative\ \gamma}$	7×10^{-4}
$\delta_{High\ Energy\ Cut}$	2×10^{-4}
$\delta_{Fiducial\ Volume}$	5×10^{-4}
δ_{Fit}	$< 1 \times 10^{-4}$
δ_{π^0}	3×10^{-4}
$\delta_{p^*_{min}}$	3×10^{-4}
$\delta_{p^*_{Max}}$	$< 1 \times 10^{-4}$
δ_{Tag}	1×10^{-4}
$\delta_{MC\ Lifetime}$	$< 10^{-6}$
$\delta_{Nuclear\ interactions}$	$< 4 \times 10^{-4}$
δ_{FILFO}	$< 3 \times 10^{-4}$
$\delta_{CRV\ and\ T3\ filter}$	$\mathcal{O}(10^{-6})$
$\delta_{Trigger\ clusters\ overlap}$	9×10^{-4}
Total systematic uncertainties	15×10^{-4}

Table 2: Summary table of systematic uncertainties. The total systematic uncertainty is obtained as square root of the sum of the square of each term.

which has to be compared with the PDG fit value for the $K \to \mu\nu_\mu$, which is 0.6343 ± 0.0017.
We can use our result for measuring $|V_{us}|$ in the Marciano's way ([7,8] and appendix):

$$|V_{us}|_{K_{\mu 2}} = 0.2223(26). \tag{29}$$

This value of V_{us} is consistent with the unitarity of the first row of the CKM matrix to 1σ. Moreover the uncertainty of this method is mainly theoretical and due to lattice calculation.
This result is in agreement with the most recent data available in literature (see figure 13).

Appendix: V_{us} from the $K_{\mu 2}$ decay

A method to obtain $|V_{us}|$ using the $K \to \mu\nu(\gamma)$ decay has been proposed by W.J.Marciano [7]. The basis of this study is the lattice calculation of f_K/f_π.

The starting point is the ratio of the calculated decay rates for the inclusive

Summary table		
	Monte Carlo	Data
Signal sample		
Number of $K^+ \to \mu^+\nu(\gamma)$	1378454	865283
Number of K^- tags	5541922	4237329
Efficiency sample		
Number of $K^+ \to \mu^+\nu(\gamma)$	1413350	1245636
Number of K^- tags	3662011	3944741
True efficiency sample		
Number of $K^+ \to \mu^+\nu(\gamma)$	2604618	
Number of K^- tags	6756201	

Table 3: Summary table of the quantities used for the measurement.

decays $\pi \to \mu\nu(\gamma)$ (called $\pi_{\mu 2}$) and $K \to \mu\nu(\gamma)$ (called $K_{\mu 2}$) which are given by [9]:

$$\frac{\Gamma(K \to \mu\nu(\gamma))}{\Gamma(\pi \to \mu\nu(\gamma))} = \frac{|V_{us}|^2 f_K^2 m_K \left(1 - \frac{m_\mu^2}{m_K^2}\right)^2}{|V_{ud}|^2 f_\pi^2 m_\pi \left(1 - \frac{m_\mu^2}{m_\pi^2}\right)^2} \times \frac{\left[1 + \frac{\alpha}{\pi} C_K\right]}{\left[1 + \frac{\alpha}{\pi} C_\pi\right]} \tag{30}$$

where G_F, m_μ, m_π, m_K are the Fermi coupling constant, the masses of muon, pion and kaon respectively. The radiative inclusive electroweak corrections in those expressions are parametrized by C_π and C_K, they include virtual loop effects as well as real bremsstrahlung emission. By convention all $\mathcal{O}(\alpha)$ effects have been factored out, so the pion and kaon form factors should be in principle independent of QED ambiguities.
Taking into account the radiative corrections, estimated by [9–13], inserting the experimental values [14], and using the latest lattice calculation [15]:

$$f_K/f_\pi = 1.210(4)(13) \tag{31}$$

we can obtain the ratio [7]:

$$\left|\frac{V_{us}}{V_{ud}}\right|^2 = 0.05211(16)(19)(117) \tag{32}$$

where the errors correspond, respectively, to the experimental, the structure dependent radiative corrections and the lattice uncertainties. Using $|V_{ud}| = 0.9740 \pm 0.0005$ from nuclear beta decays [8] it is possible to determine:

$$|V_{us}|_{K_\mu 2} = 0.2223(26) \tag{33}$$

The accuracy is dominated by the knowledge of f_K/f_π from lattice calculation.
Alternatively, the unitarity relationship $|V_{ud}|^2 = 1 - |V_{us}|^2$ can be assumed in eq. 32

giving:

$$|V_{us}|_{unitarity} = 0.2225(25) \tag{34}$$

independent of the V_{ud} measurement.
The obtained result quoted in eq. 33 is in agreement with the unitarity of the CKM matrix and with the determinations of V_{us} from semileptonic decays, dominated by the $f_+(0)$ calculations.

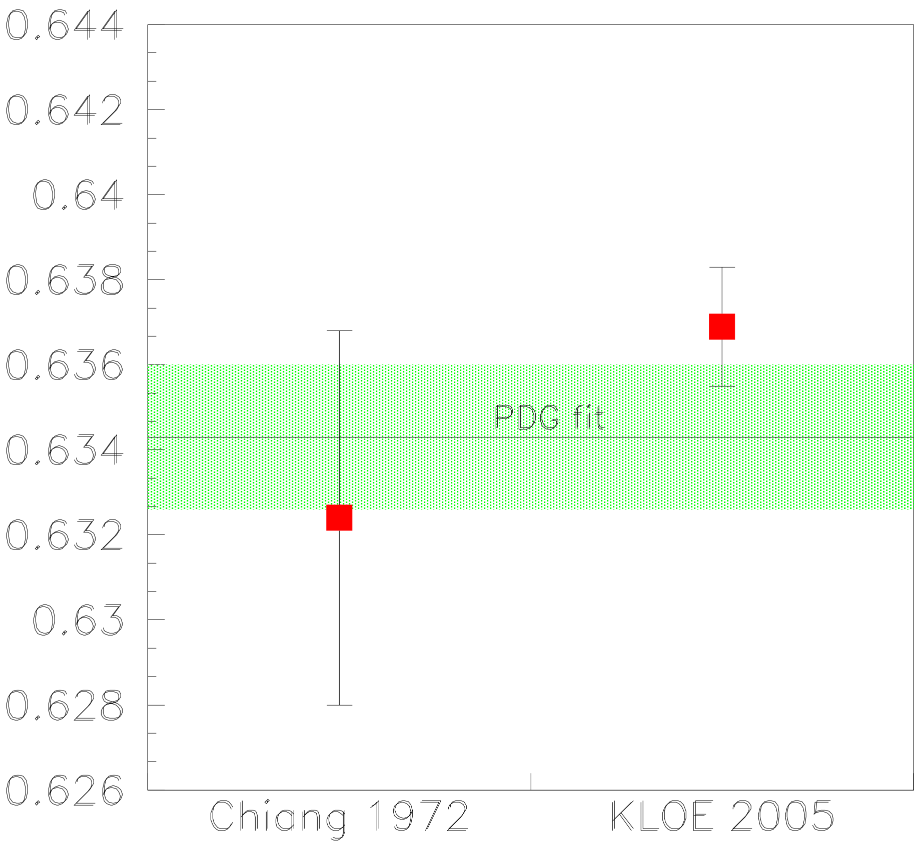

Figure 12: Comparison between the $K \to \mu\nu$ branching ratio available in literature and our result.

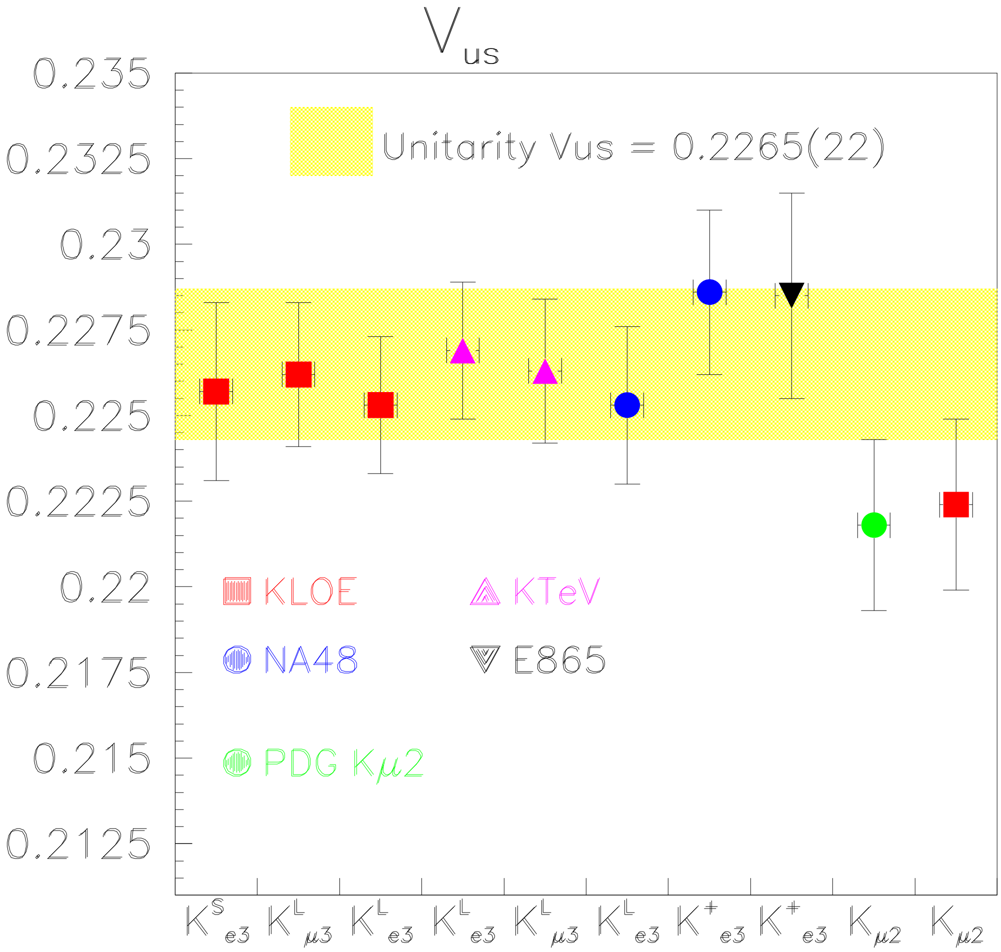

Figure 13: Summary table of V_{us} with the most recent measurements plus our result.

References

[1] S. Eidelman *et al.* [Particle Data Group Collaboration], Phys. Lett. B **592** (2004) 1.

[2] I. H. Chiang, J. L. Rosen, S. Shapiro, R. Handler, S. Olsen and L. Pondrom, Phys. Rev. D **6** (1972) 1254.

[3] see the review on "The Cabibbo-Kobayashi-Maskawa quark-mixing matrix" S. Eidelman *et al.* [Particle Data Group], Phys. Lett. B **592** (2004).

[4] M. Adinolfi *et al.* [KLOE Collaboration], Nucl. Instrum. Meth. A **492** (2002) 134.

[5] C. Bini et al., *Rejection of cosmic rays and Bhabha background with the electromagnetic calorimeter*, KLOE Memo **126** (1997); B. Golosio et al., *Rejection of machine background in the KLOE experiment*, KLOE Memo **172** (1998); G. Finocchiaro, A. Menicucci, *Cosmic rays rejection in KLOE*, KLOE Memo **203** (1999); G. Finocchiaro, A. Menicucci, *Machine background rejection in KLOE*, KLOE Memo **204** (1999).

[6] V. S. Demidov, V. A. Dobrokhotov, E. A. Lyublev and A. N. Nikitenko, Sov. J. Nucl. Phys. **52** (1990) 1006 [Yad. Fiz. **52** (1990) 1595].

[7] W. J. Marciano, Phys. Rev. Lett. **93** (2004) 231803

[8] A. Czarnecki, W. J. Marciano and A. Sirlin, Phys. Rev. D, Vol.70 (2004) 093006

[9] W. J. Marciano and A. Sirlin, Phys. Rev. Lett. **71** (1993) 3629.

[10] W. J. Marciano and A. Sirlin, Phys. Rev. Lett. **56** (1986) 22.

[11] A. Sirlin, Rev. Mod. Phys. **50** (1978) 573 [Erratum-ibid. **50** (1978) 905].

[12] T. Kinoshita, Phys. Rev. Lett. **2** (1959) 477.

[13] M. Finkemeier, Phys. Lett. B **387** (1996) 391 [arXiv:hep-ph/9505434].

[14] K. Hagiwara *et al.* [Particle Data Group Collaboration], Phys. Rev. D **66** (2002) 010001.

[15] C. Aubin *et al.* [MILC Collaboration], Phys. Rev. D **70**, 114501 (2004)